Title: Dynamin-related protein Drp1 and mitochondria are important for *Shigella flexneri* infection

Author: Mabel Lum Renato Morona

PII: S1438-4221(14)00027-7
DOI: http://dx.doi.org/doi:10.1016/j.ijmm.2014.03.006
Reference: IJMM 50808

To appear in:

Received date: 5-2-2014
Revised date: 17-3-2014
Accepted date: 24-3-2014

Please cite this article as: Lum, M., Morona, R.,Dynamin-related protein Drp1 and mitochondria are important for *Shigella flexneri* infection, *International Journal of Medical Microbiology* (2014), http://dx.doi.org/10.1016/j.ijmm.2014.03.006

Title: Dynamin-related protein Drp1 and mitochondria are important for *Shigella flexneri* infection

Authors: Mabel Lum, Renato Morona*

Address: School of Molecular and Biomedical Science, University of Adelaide, Adelaide, South Australia, Australia

Contact details:

* E-mail: renato.morona@adelaide.edu.au

Tel: 61 8 8313 4151

Fax: 61 8 8313 7532

Abstract

Shigella infection in epithelial cells induces cell death which is accompanied by mitochondrial dysfunction. In this study the role of the mitochondrial fission protein, Drp1 during *Shigella* infection in HeLa cells was examined. Significant lactate dehydrogenase (LDH) release was detected in the culture supernatant when HeLa cells were infected with *Shigella* at a high multiplicity of infection. Drp1 inhibition with Mdivi-1 and siRNA knockdown significantly reduced LDH release. HeLa cell death was also accompanied by mitochondrial fragmentation. Tubular mitochondrial networks were partially restored when Drp1 was depleted with either siRNA or inhibited with Mdivi-1. Surprisingly either Mdivi-1 treatment or Drp1 siRNA-depletion of HeLa cells also reduced *Shigella* plaque formation. The effect of Mdivi-1 on *Shigella* infection was assessed using the murine Sereny model, however it had no impact on ocular inflammation. Overall our results suggest that Drp1 and the mitochondria play important roles during *Shigella* infection.

Keywords:

Shigella flexneri

Cell death

Cell spreading

Drp1

Mitochondria

Mdivi-1

Introduction

Shigella flexneri is the causative agent of bacillary dysentery (shigellosis) and is a significant human pathogen due to its high morbidity among children < 5 years in developing countries (Bardhan et al., 2010). The key pathogenic features of *Shigella* include cell death induction in myeloid immune cells and circumventing cell death in colonic epithelial cells, the site of *Shigella* infection. *Shigella* also interact with host proteins to initiate de novo actin synthesis to facilitate its intra- and intercellular spread to disseminate within the colon.

Post ingestion of contaminated food and water, *Shigella* initially invades the host intestinal epithelium via microfold cells and induce pyroptosis of the resident macrophages in the follicle associated epithelium by activating ICE protease-activating factor-dependent (IPAF/NLRC4) and apoptosis-associated speck-like protein containing caspase recruitment domain (ASC) inflammasome (Senerovic et al., 2012; Suzuki et al., 2007). Subsequent caspase-1 activation releases interleukin-1β (IL-1β) and interleukin-18 (IL-18), resulting in strong inflammatory responses and magnified innate responses, respectively (Sansonetti et al., 2000). Another form of necrotic cell death induced in macrophage is pyronecrosis, which is independent of caspase-1 activation and releases another proinflammatory factor, HMGB1 (high-mobility group box 1 protein) (Willingham et al., 2007).

Following macrophage pyroptosis, *Shigella* are released into the basolateral compartment and invade enterocytes via the type three secretion system (TTSS), followed by lysis of the endocytic vacuole and replication in the cytoplasm (Cossart and Sansonetti, 2004; Sansonetti et al., 1986). The polarly localised *Shigella* IcsA protein interacts with the host N-WASP (Neural Wiskott-Aldrich syndrome protein) and Arp2/3 complex to initiate F-actin nucleation and polymerisation, leading to actin based motility which allows the bacterium to spread within the cytoplasm and also laterally via protrusion formation into the adjacent cells (Bernardini et al., 1989; Lett et al., 1989; Makino et al., 1986). After escaping from the double membrane vacuole, subsequent cycles of infection are initiated (Schuch et al., 1999). Proteins localised at the enterocyte tight junctions and adherens junctions facilitate *Shigella* protrusion formation and may associate directly with the *Shigella* actin tail (Bishai et al., 2012; Kadurugamuwa et al., 1991; Sansonetti et

al., 1994). *Shigella* invasion and dissemination is also dependent on ATP release by connexion 26 and formins, Dia1 and Dia2, which can initiate de novo actin polymerisation and crosslink actin filaments (Heindl et al., 2009; Tran Van Nhieu et al., 2003). Components of the clathrin mediated endocytosis pathway also facilitate *Shigella* entry into the adjacent cell (Fukumatsu et al., 2012; Lum et al., 2013).

Eliminating infected enterocytes prevents *Shigella* from propagating and disseminating into uninfected cells (Ashida et al., 2011). However *Shigella* is able to delay cell death by manipulating host signalling pathways. Depending on the experimental conditions such as host cell type, time of infection and multiplicity of infection (moi), apoptotic and necrotic cell death have been observed during *Shigella* infection. Apoptosis is a non-inflammatory cell death which is activated by mitochondria and death receptor mediated pathways characterised by caspase activation, DNA fragmentation, cell shrinkage, membrane blebbing and mitochondrial permeability (Lamkanfi and Dixit, 2010), whereas necrosis is characterised by nuclear swelling, membrane rupture and spillage of cellular contents into the environment resulting in inflammatory conditions. Absence of caspase activation, reactive oxygen species (ROS) production, lysosomal destabilization, calpain release and ATP depletion are also observed (Golstein and Kroemer, 2007; Vandenabeele et al., 2010).

S*higella* infection in HeLa cells induces an early genotoxic stress (Bergounioux et al., 2012). The tumour suppressor protein p53, an inducer of apoptosis is normally stabilised during genotoxic response. However p53 is rapidly degraded by calpain, through degradation of the calpain protease inhibitor, calpastatin, by the *Shigella* VirA TTSS effector (Bergounioux et al., 2012). Calpain activation inadvertently activates the necrosis pathway which restricts *Shigella* intracellular growth (Bergounioux et al., 2012). In the colonic HCT116 cells, the slow degradation of p53 shifts the executing pathway from necrosis to apoptosis (Bergounioux et al., 2012). In HaCat (immortalized keratinocytes) cells, the *Shigella* TTSS effector, OspC3 targets the p19 subunit of Caspase-4 to delay necrotic cell death (Kobayashi et al., 2013). In vivo the Δ*ospC3* mutant exacerbates colonic inflammation in guinea pigs (Kobayashi et al., 2013). In HeLa cells and mouse embryonic fibroblasts (MEFs), pro-survival Nod1/NF-κB/Bcl-2 signalling is activated to counteract the necrotic pathway mediated by Bnip3, a regulator of mitochondrial

permeability transition during *Shigella* infection (Carneiro et al., 2009). In staurosporine (STS)-induced apoptosis in HeLa cells, the *Shigella* Spa15 (TTSS) effector prevented caspase-3 activation (Faherty and Maurelli, 2009). *Shigella* infection in HeLa cells and in an ex vivo colonic epithelial cell model reportedly triggered apoptosis via caspase-9 and caspase-3 activation (Lembo-Fazio et al., 2011). Furthermore Gadd45a (stress sensor growth arrest and DNA damage 45a), a stress-inducible gene, was also upregulated in vitro and ex vivo (Lembo-Fazio et al., 2011).

Mitochondrial fission is an important downstream event for intrinsic apoptotic and programmed necrosis signalling pathways (Otera et al., 2013). Mitochondrial constriction is initially mediated by the endoplasmic reticulum and actin (Friedman et al., 2011; Korobova et al., 2013). Dimeric or tetrameric cytosolic dynamin-related protein 1 (Drp1, also known as dynamin-1-like protein) is then recruited to fission sites on the mitochondria to its receptor, Mff (Otera et al., 2010). In the presence of GTP, Drp1 self-assembly stimulates GTP hydrolysis and formation of higher order structures as foci at the mitochondrial fission sites (Smirnova et al., 2001). Oligomerised Drp1 wraps around the mitochondria and following GTP hydrolysis, the mitochondrial membrane is severed (Smirnova et al., 2001). Drp1 assembly on the mitochondria is inhibited by the small molecule inhibitor, mitochondrial division inhibitor-1 (Mdivi-1) through interactions with an allosteric site which does not affect its GTPase activity (Cassidy-Stone et al., 2008). Mdivi-1 has therapeutic effects in various animal models of non-infectious diseases (Ferrari et al., 2011; Ong et al., 2010; Tang et al., 2013).

Previously we reported that dynasore, an inhibitor of dynamin II and Drp1 GTPase activity affected *Shigella* cell spreading and *Shigella*-induced cytotoxicity in HeLa cells. Furthermore dynasore also protected mice from weight loss in an ocular infection model even though inflammation was not reduced (Lum et al., 2013). We decided to investigate if Drp1 contributed to the observations we made earlier. In this study HeLa cells were infected with *Shigella* at a moi (multiplicity of infection) of 500 and 1000. During *Shigella* infection, lactate dehydrogenase (LDH) was released into the culture supernatant. HeLa cells treated with a pan-caspase inhibitor did not reduce LDH release and caspase-3 was not activated, suggesting *Shigella* induces non-apoptotic cell death under these conditions. Drp1 inhibition with Mdivi-1 and Drp1 depletion

with siRNA reduced LDH release. Mitochondrial fragmentation was also observed in *Shigella*-infected cells and was partially restored when HeLa cells were either treated with Mdivi-1 or when Drp1 was depleted with siRNA. Unexpectedly *Shigella* plaque formation was reduced in Mdivi-1-treated HeLa cells. This was also observed in HeLa cells knockdown with Drp1 siRNA, suggesting maintaining mitochondria structure is important for efficient cell spreading. A murine Sereny test was used to determine if Mdivi-1 could reduce keratoconjunctivitis or protect mice from weight loss due to *Shigella* infection. Mdivi-1 treatment did not reduce ocular inflammation but did protect mice from weight loss in the first 24 h only. These results suggest Drp1 and the mitochondria are critical for *Shigella* infection.

Materials and methods

Bacterial strains and growth media

The strains used in this study are listed in Table 1. *S. flexneri* strains were grown from a Congo Red positive colony as described previously (Morona et al., 2003) and were routinely cultured in Luria Bertani (LB) broth and on LB agar. Virulence plasmid-cured (VP^-) derivative of WT *S. flexneri* strain was isolated on Congo Red agar as white colonies and re-streaked until pure (Morona and Van Den Bosch, 2003). Bacteria were grown in media for 16 h with aeration, subcultured 1/20 and then grown with aeration to mid-exponential growth phase for 1.5 h at 37°C. Where appropriate, media were supplemented with tetracycline (4 or 10 μg/mL).

Chemicals and antibodies

IM-54 (5 mM stock - ALX-430137; Enzo Life Sciences), Mdivi-1 (50 mM stock - M0199; Sigma-Aldrich, BML-CM127; Enzo Life Sciences), Necrostatin-1 (100 mM stock - N9037; Sigma-Aldrich), Necrostatin-7 (20 mM stock - ALX-430-170; Enzo Life Sciences), Necrosulfonamide (20 mM stock - N388600; Toronto Research Chemicals), NecroX-2 (5 mM stock - ALX-430-166; Enzo Life Sciences), NecroX-5 (5 mM stock - ALX-430-167; Enzo Life Sciences), Staurosporine (10 mM stock - 00025, Biotium), Z-FA-FMK (20 mM stock - 550411; BD Biosciences) and Z-VAD-fmk (20 mM stock - Merck Calbiochem; 627610) were prepared in dimethyl sulfoxide (DMSO) (D2650; Sigma-Aldrich) for in vitro studies. For in vivo studies, Mdivi-1 was dissolved in a formulation containing 1-methyl-2-pyrrolidione (NMP/Pharmasolve; Ashland ISP) and polyethylene glycol 300 (PEG300; Sigma-Aldrich) (1 part NMP to 9 parts

PEG300). Mdivi-1 was prepared as a 22 mg/mL stock and diluted 1/4 (5.5 mg/mL) with NMP/PEG before injection into mice. Mouse anti-DLP1 antibody (611112; BD Biosciences) and rabbit anti-GAPDH antibody (600-401-A33; Rockland Immunochemicals, Inc.) were used at 1:100 and 1:3000 for Western immunoblotting, respectively. For immunofluorescence (IF) microscopy, rabbit anti-active (cleaved) caspase-3 antibody (AB3623; Merck Milipore), anti-DLP1 antibody, Alexa 594-conjugated donkey anti-mouse secondary antibody and Alexa Fluor 594-conjugated donkey anti-rabbit antibody (Molecular Probes) were used at 1:100.

Reverse transfection and HeLa cell lysate preparation

DNM1L siRNA (L012092-00-0005) and siRNA controls (Non-targeting Pool; D-001810-10-05, siGLO Green Transfection Indicator; D-001630-01-05) were purchased from Thermo Scientific. siRNAs were transfected with DharmaFECT 3 Transfection Reagent (T-2003-03) and DharmaFECT Cell Culture Reagent (DCCR; B-004500-100), also purchased from Thermo Scientific. Reverse transfection of HeLa cells (Human, cervical, epithelial cells ATCC #CCL-70) were carried out based on a method by Thermo Scientific. siRNA were prepared as a 5 μM stock and the final concentration used was 50 nM. HeLa cells were transfected and cell lysates were prepared as described previously (Lum et al., 2013).

SDS-PAGE and Western immunoblotting

SDS-PAGE (12% acrylamide gel) and Western immunoblotting were carried out as described previously (Lum et al., 2013). Molecular weight markers used were BenchMark™ Pre-Stained Protein Ladder (Invitrogen).

Plaque assay

Plaque assays were performed with HeLa cells as described previously by Oaks *et al.* (Oaks et al., 1985) with modifications. HeLa cells were transfected in 12-well trays prior to plaque assay as described previously (Lum et al., 2013). On day 4, the plaque assay was carried out when the cells reached confluency. HeLa cells were washed twice with Dulbecco's modified Eagle medium (DMEM) prior to inoculation. 5×10^4 mid-exponential phase bacteria were added to each well. Trays were incubated at 37°C, 5% CO_2 and were rocked gently every 15 min to spread the inoculum evenly across the well. At 90 min post infection, the inoculum was

aspirated. 0.5 mL of the first overlay (DMEM, 5% FCS, 20 µg/mL gentamicin, 0.5% (w/v) agarose [Seakem ME]) was added to each well. The second overlay (DMEM, 5% FCS, 20 µg/mL gentamicin, 0.5% (w/v) agarose, 0.1% (w/v) Neutral Red solution [Gibco BRL]) was added 24 h post infection and plaques were imaged 6 h later. All observable plaques were counted and the diameter was measured for each condition in each experiment. At least 50 plaques were measured for each condition.

Infectious focus assay

1.2×10^6 HeLa cells were seeded in six-well trays in minimal essential medium (MEM), 10% FCS, 1% penicillin/streptomycin. Cells were grown to confluence overnight and were washed twice with DMEM prior to inoculation. 5×10^4 mid-exponential phase bacteria expressing mCherry were added to each well. Trays were incubated at 37°C, 5% CO_2 and were rocked every 15 min to spread the inoculum evenly across the well. At 90 min post infection, the inoculum was aspirated. 1.5 mL of DMEM (phenol red-free) (31053-028; Life Technologies), 1 mM sodium pyruvate, 5% FCS, 20 µg/mL gentamicin, 2 mM IPTG was added to each well. Mdivi-1 or DMSO were added and were swirled to ensure even distribution. 24 h later the infectious foci were imaged with an Olympus IX-70 microscope using a 10× objective. The filter set used was DA/FI/TX-3X-A-OMF (Semrock). Fluorescence and phase contrast images were captured and false colour merged with the Metamorph software program (Version 7.7.3.0, Molecular Devices). The area of the infectious focus, i.e. area where mCherry was expressed, was outlined and measured with Metamorph. All observable infectious foci were counted and the area was measured for each condition in each experiment. At least 5 infectious foci were measured for each condition.

Invasion assay and IF microscopy

HeLa cells (8×10^4) were seeded onto sterile glass cover slips in 24-well trays in MEM, 10% FCS, 1% penicillin/streptomycin. For transfected cells, HeLa cells were transfected as described previously (Lum et al., 2013). Cells were grown to semi-confluence overnight, washed twice with Dulbecco's PBS (D-PBS) and once with MEM, 10% FCS. 4×10^7 mid-exponential phase bacteria were added to each well and subsequently centrifuged (2,000 rpm, 7 min, Heraeus Labofuge 400 R) onto HeLa cells. After 1 h incubation at 37°C, 5% CO_2, the infected cells were

washed thrice with D-PBS and incubated with 0.5 mL MEM containing 40 µg/mL of gentamicin for a further 1.5 h (or 3.5 h for labelling with anti-activated caspase-3). Infected cells were washed thrice in D-PBS, fixed in 3.7% (v/v) formalin for 15 min, incubated with 50 mM NH_4Cl in D-PBS for 10 min, followed by permeabilisation with 0.1% Triton X-100 (v/v) for 5 min. After blocking in 10% FCS in PBS, the infected cells were incubated at 37°C for 30 min with the desired primary antibody. After washing in PBS, coverslips were incubated with either Alexa Fluor 594-conjugated donkey anti-mouse or Alexa 594-conjugated donkey anti-rabbit secondary antibody (Molecular Probes) (1:100). F-actin was visualised by staining with Alexa Fluor 488-conjugated phalloidin (2 U/mL) and 4',6'-diamidino-2-phenylindole (DAPI) (10 µg/mL) was used to counterstain bacteria and HeLa cell nuclei. Coverslips were mounted on glass slides with Mowiol 4-88 (Calbiochem) containing 1 µg/mL *p*-phenylenediamine (Sigma) and was imaged using a 100× oil immersion objective (Olympus IX-70). The filter set used was DA/FI/TX-3X-A-OMF (Semrock). Fluorescence and phase contrast images were false colour merged using the Metamorph software program.

MitoTracker® Red CMXRos labelling

HeLa cells were seeded and infected as described in "***Invasion assay and IF microscopy***". The infected cells were washed thrice with D-PBS and incubated with 0.5 mL MEM containing 40 µg/mL of gentamicin for 2 h 55 min. The media was removed and replaced with pre-warmed 400 nM MitoTracker® Red CMXRos (Invitrogen) in MEM, 40 µg/mL gentamicin for 35 min. HeLa cells were washed thrice with pre-warmed D-PBS, fixed in pre-warmed 3.7% (v/v) formalin for 15 min, followed by three washes with pre-warmed PBS. Bacteria and HeLa cell nuclei were stained with 10 µg/mL DAPI in MQ water for 1.5 min at RT, followed by two washes with pre-warmed PBS and one wash with pre-warmed mQ water. Cover slips were mounted and imaged using a 100× oil immersion objective as described in ***"Invasion assay and IF microscopy"***.

Protrusion formation

HeLa cells were seeded, infected and fixed as per ***"Invasion assay and IF microscopy"***. HeLa cells were washed twice with 1× Annexin V binding buffer (99902; Biotium) prepared in milliQ (18.2 MΩ·cm) water, mounted on glass slides with the same buffer and were imaged using a 40× oil immersion objective (Olympus IX-70). Protrusion formation was defined as any extensions of

bacterial projection(s) (minimum of a full bacterial length) beyond the periphery of the HeLa cell. For each condition in each experiment, a minimum of 100 cells were imaged.

Assay for growth of intracellular bacteria

HeLa cells (8×10^4) were seeded in 24-well trays in MEM, 10% FCS, 1% penicillin/streptomycin. Cells were grown to semi-confluence overnight, washed twice with D-PBS and once with MEM, 10% FCS. 4×10^7 mid-exponential phase bacteria were added to each well (moi 500) and were centrifuged (2,000 rpm, 7 min, Heraeus Labofuge 400 R) onto HeLa cells. After 1 h incubation at 37°C, 5% CO_2, the infected cells were washed thrice with D-PBS and incubated with 0.5 mL MEM containing 40 µg/mL of gentamicin. At the indicated intervals, monolayers (in duplicate) were washed four times in D-PBS and were lysed with 0.1% (v/v) Triton X-100 in PBS for 5 min and bacteria were enumerated on tryptic soy agar (TSA; Gibco) plates.

LDH cytotoxicity assay

HeLa cells (3×10^4) were seeded in 96-well trays in MEM, 10% FCS, 1% penicillin/streptomycin. Cells were grown to confluence overnight and were washed twice with PBS. 50 µL phenol-red free DMEM, 1 mM sodium pyruvate and 3×10^7 mid-exponential phase bacteria (moi 1000) in 50 µL PBS or PBS were added into each well, where appropriate. The bacteria were centrifuged (2,000 rpm, 7 min, Heraeus Labofuge 400 R) onto HeLa cells. After 1 h incubation at 37°C, 5% CO_2, the infected cells were washed thrice with PBS and incubated with 0.1 mL phenol-red free MEM, 40 µg/mL of gentamicin for 4 h. LDH activity was measured with the Cytotoxicity Detection Kit^{Plus} as per manufacturer's instructions (Roche). The percentage of LDH released was calculated with the following formula: ((experimental LDH release − spontaneous LDH release) / (maximal LDH − spontaneous LDH release)) × 100.

Ethics statement

The use of animals in this study has been approved by the University of Adelaide Animal Ethics Committee (Project number: S-2012-90). All animals used were handled in compliance with the Australian code of practice for the care and use of animals for scientific purposes, 7th edition (2004).

284

285 **Mouse Sereny test**

286 The mouse Sereny test (Murayama et al., 1986) was carried out as described previously (Lum et
287 al., 2013). Male Balb/c mice (20-22g) were inoculated with 2.5×10^7 CFUs bacteria in 5 µL of
288 bacterial suspension (in PBS) into the right eye; the left eye served as a diluent control. To
289 ascertain the impact of Mdivi-1 on ocular infection, mice were injected intraperitoneally (IP)
290 with drug at a dose rate of 30 mg/kg, at t = -1, +6, +23 and +30 hours with respect to infection at
291 0 hours. Keratoconjunctivitis was evaluated at specific time points after inoculation and scored
292 on a scale ranging from 0 (no infection), 1 (mild keratoconjuctivitis where the eye lid is slightly
293 swollen), 2 (severe keratoconjuctivitis where the eye is half closed) and 3 (fully developed
294 keratoconjunctivitis where the eye is completely closed). Due to an ethics concern with the in
295 vivo use of DMSO, Mdivi-1 was prepared in NMP/PEG, which is made up of 1 part 1-methyl-2-
296 pyrrolidione (NMP) and 9 parts polyethylene glycol 300 (PEG300). A preliminary mouse study
297 showed that this dosing regime resulted in 10% weight loss over a period of 72 h (Fig. S1).

298

299 **Statistical analysis**

300 Statistical analysis was carried out using GraphPad Prism 6. Results are expressed as means ±
301 SEM of data obtained in independent experiments. Statistical differences between two groups
302 were determined with a two-tailed unpaired *t*-test. Statistical differences between three or more
303 groups were determined with a one-way ANOVA followed by Tukey's multi comparison post
304 hoc test. Statistical significance was set at $p < 0.05$.

305

306 **Results**

307 ***S. flexneri* induces Drp1-mediated cell death in HeLa cells**

308 In a preliminary experiment, we investigated the effects of *S. flexneri* moi on LDH release. HeLa
309 monolayers were infected with WT or virulence plasmid-cured (VP^-) *S. flexneri* at moi ranging
310 from 1 - 1000 (Fig. S2). HeLa cells infected with WT *Shigella* at moi of ≥ 100 had significantly
311 higher LDH release compared to the VP^- strain. Moi of 500 and 1000 was used in this study to
312 reflect the experimental conditions used previously (Lum et al., 2013). No difference in LDH
313 release was observed between moi 500 and 1000 (Fig. S2).

314

Recently we reported that dynasore, a non-competitive, reversible inhibitor of dynamin II and Drp1 GTPase activity significantly reduced *S. flexneri*-induced cytotoxicity in HeLa cells (Lum et al., 2013). The efficacy of dynasore was also tested in a murine ocular infection model. Mice treated with dynasore lost significantly less weight compared to mice treated with the NMP/PEG vehicle, however no improvement in ocular inflammation was observed. These results prompted us to examine the role of Drp1, if any, during *S. flexneri* pathogenesis. We initially investigated if *S. flexneri*-induced HeLa cytotoxicity was mediated by the mitochondrial fission protein, Drp1. The effects of Mdivi-1, a Drp1 inhibitor, and Drp1 siRNA on LDH release were determined. HeLa monolayers infected with *S. flexneri* (moi 1000) were treated with increasing concentrations of Mdivi-1 or with the DMSO control alone. *Shigella*-infected DMSO-treated HeLa cells released high levels of LDH (43.68 ± 0.85%). In HeLa cells treated with 50 μM Mdivi-1, LDH release was significantly reduced (32.70 ± 0.47%) and further reduction was observed with 100 μM Mdivi-1 treatment (24.06 ± 2.70) (Fig. 1A). To investigate the effect of Drp1 depletion on *S. flexneri*-induced cytotoxicity, HeLa cells were transfected with Drp1 siRNA and LDH release by infected cells was measured. Western immunoblots of HeLa cell lysates two days post siRNA treatment showed no detectable Drp1 levels (Fig. 1B). LDH release induced by *S. flexneri* was significantly reduced in HeLa cells treated with Drp1 siRNA (*$p < 0.05$) (Fig. 1C).

<u>*S. flexneri* induces non-apoptotic cell death in HeLa cells</u>

Since Drp1 have been implicated in both apoptosis and necrosis, we determined if components of the apoptotic or necrotic cell death pathways were involved. Uninfected HeLa monolayers were treated with the DMSO control or positive control agents; staurosporine (STS) to induce apoptosis or 0.01% Triton X-100 to induce necrosis (Kwon et al., 2011) (Fig. 2A). LDH release was observed in HeLa cells treated with 0.01% Triton X-100 but not STS. The effects of Z-VAD-fmk, a pan-caspase inhibitor and its inactive analogue, Z-FA-fmk, on LDH release during *S.flexneri* infection were determined. HeLa monolayers infected with *S. flexneri* were treated with increasing concentrations of Z-VAD-fmk or Z-FA-fmk or the DMSO control. No reduction in LDH release was observed (Fig. 2B and 2C). Caspase-3 cleavage is indicative of apoptosis activation (Reed, 2000). We investigated activated caspase-3 localisation in untreated, DMSO-treated, STS-treated and *S. flexneri*-infected (moi 500) HeLa cells (Fig. S3A - 3D). Activated

caspase-3 was only observed in HeLa cells treated with STS (Fig. S3C). Nuclear and cell shrinkage was also observed. Therefore *S. flexneri* infection induced non-apoptotic cell death in HeLa cells. Since LDH release was observed when HeLa cells were treated with Triton X-100 and not STS, we reasoned that the cell death pathway activated during *Shigell*a infection under the conditions used is most likely necrosis.

Next we investigated if components of the programmed necrosis pathway are important during *S. flexneri*-infection. Necrostatin-1 is an allosteric inhibitor of receptor-interacting Ser/Thr kinases 1 (RIP1) (Degterev et al., 2008); necrostatin-7 targets an unknown effector in the programmed necrosis pathway (Zheng et al., 2008) and necrosulfonamide covalently modifies mixed lineage kinase domain-like protein (MLKL) to prevent downstream necrosis activation (Sun et al., 2012). HeLa monolayers infected with *S. flexneri* (moi 1000) were treated with increasing concentrations of necrostatin-1 or necrostatin-7 or necrosulfonamide or with the DMSO control alone. No reduction in LDH release was observed (Fig. 2D, 2E and 2F). We also investigated if *S. flexneri*-induced cell death was a result of oxidative stress. IM-54 inhibits hydrogen peroxide-induced necrosis (Dodo et al., 2005); and NecroX-2 and NecroX-5 are mitochondria-targeted ROS and nitrogen oxidative species (NOS) scavengers (Kim et al., 2010). HeLa monolayers infected with *S. flexneri* (moi 1000) were treated with increasing concentrations of IM-54 or NecroX-2 or NecroX-5 or with the DMSO control alone. No reduction in LDH release was observed (Fig. 2G and 2H). Hence *S. flexneri*-induced cell death in HeLa cells is unlikely a consequent of oxidative stress and is unlikely activated via the RIP1/MLKL programmed necrosis pathway.

<u>*S. flexneri* infection induces mitochondrial fragmentation</u>

Next we investigated the effects of *S. flexneri* infection on mitochondria of HeLa cells by IF microscopy. In uninfected and DMSO-treated HeLa cells, the mitochondrial network is long and tubular (Fig. 3A and 3B). When mitochondrial division is inhibited, tubular mitochondrial networks becomes interconnected to form net-like structures, or collapse into perinuclear structures (Smirnova et al., 2001; Smirnova et al., 1998). HeLa cells treated with the Drp1 inhibitor, Mdivi-1, had degenerate perinuclear mitochondrial structures (Fig. 3C). HeLa cells were either untreated, treated with DMSO or treated with Mdivi-1, and were infected with *S.*

flexneri (moi 500) for 3.5 hours. Infected HeLa cells treated with Mdivi-1 had significantly reduced mitochondrial fragmentation (17.26 ± 1.26%) compared to untreated (33.49 ± 3.40%) or DMSO-treated (30.88 ± 1.63%) HeLa cells (Fig. 3D - 3G). High bacterial loads were also observed in *Shigella*-infected HeLa cells regardless of treatment (Fig. 3D - 3F).

The effect of Drp1 depletion on mitochondrial fragmentation during *S. flexneri* infection was determined. HeLa cells were mock transfected or transfected with either negative siRNA or Drp1 siRNA, and were infected with *S. flexneri* (moi 500) for 3.5 hours. Drp1-depleted HeLa cells had significantly reduced mitochondrial fragmentation (15.94 ± 2.55%) compared with mock-transfected (27.65 ± 0.38%) or negative siRNA-treated (27.88 ± 0.10%) HeLa cells during *Shigella* infection (Fig. 4A - 4D). No differences in bacterial loads were observed in infected cells regardless of treatment. Therefore *S. flexneri* infection in HeLa cells increased Drp1 dependent mitochondrial fragmentation.

Drp1 is important for *S. flexneri* cell to cell spreading but not protrusion formation

Dynasore, an inhibitor of dynamin II and Drp1 GTPase reduced *S. flexneri* cell to cell spreading. Dynamin II knockdown with siRNA also significantly affected *S. flexneri* infectious foci formation (Lum et al., 2013). We decided to investigate if Drp1 also played a role during *S. flexneri* cell to cell spreading. The effects of Mdivi-1 and Drp1 siRNA on infectious foci or plaque formation by *S. flexneri* were determined. Initial experiment showed that Mdivi-1 could not be used in the plaque assay due to precipitation when dissolved in the agar mixture. HeLa monolayers infected with *S. flexneri* (moi 0.1) were treated with increasing concentrations of Mdivi-1 in an infectious focus assay. Treatment with 20 μM Mdivi-1 reduced foci counts and foci area (*$p < 0.05$) (Fig. 5A - 5C). To investigate the effect of Drp1 depletion on *S. flexneri* cell to cell spreading, HeLa cells were transfected with Drp1 siRNA and plaque assay was carried out. *S. flexneri* formed plaques on HeLa cells treated with Drp1 siRNA with a reduced plaque diameter but not plaque counts when compared to HeLa cells treated with the negative control siRNA (*$p < 0.05$) (Fig. 6A - 6C). Therefore Drp1 inhibition with Mdivi-1 as well as siRNA knockdown reduced *Shigella* cell to cell spreading.

Reduced or absence of protrusion formation may account for decreased infectious focus and plaque formation. The role of Drp1 in *S. flexneri* protrusion formation was investigated. HeLa monolayers infected with *S. flexneri* were treated with the DMSO control or 50 μM Mdivi-1 and the percentage of infected cells with one or more bacteria protrusions were enumerated by counting >100 cells in each experiment (Fig. 7A and 7B). 55.40 ± 1.48% of infected HeLa cells had one or more protrusions. Protrusion formation was not affected by the DMSO control (55.27 ± 2.89%) or 50 μM Mdivi-1 (53.51 ± 0.06%). Reduced *S. flexneri* intracellular growth could also account for the reduction in focus area and plaque size, but no differences in bacterial counts were observed between DMSO and Mdivi-1-treated HeLa cells (Fig. S4).

Drp1 is not localised to the F-actin tails

Host proteins have been shown to associate with *S. flexneri* actin tail (Kadurugamuwa et al., 1991; Lum et al., 2013; Sansonetti et al., 1994). We investigated Drp1 localisation in *S. flexneri*-infected HeLa cells by IF microscopy. Drp1 was not localised to the *S. flexneri* actin tail in untreated, DMSO-treated, Mdivi-1-treated or Drp1 siRNA-treated HeLa cells (Fig. 8A - 8D).

Effect of Mdivi-1 on *S. flexneri* infection of mice

We next investigated the possible in vivo relevance of the observed association between Drp1 and *S. flexneri* cytotoxicity as well as cell to cell spreading. A mouse Sereny test we established previously (Lum et al., 2013) was used to determine whether ocular infection by *S. flexneri* could be inhibited by the administration of Mdivi-1. Mice in two groups were injected IP with Mdivi-1 (30 mg/kg) or vehicle at t = -1, 6, 23 and 30 h, and infected with 2.5×10^7 CFUs *S. flexneri* 2457T in the right eye (t = 0). The mice in both groups developed ocular inflammation at a similar rate and the Sereny scores were similar (Fig. S5A and S5B). Although a slight effect on weight loss was observed on D1, no differences were observed on D2 and D3 (Fig. S5C).

Discussion

Shigella infection in epithelial cells is an interplay between maintaining a replicative niche for *Shigella* and elimination of infected cells to prevent further cell spreading, even though cell death and the ensuing inflammation are at considerable cost to the host (Ashida et al., 2011). During *Shigella* infection, apoptotic (Lembo-Fazio et al., 2011) or necrotic cell death

(Bergounioux et al., 2012; Carneiro et al., 2009; Kobayashi et al., 2013) occurs depending on the experimental conditions. In both cases changes to the outer or inner mitochondrial membrane are critical to allow the respective cell death pathways to proceed. In this study we investigated the role of Drp1, the mitochondrial fission protein, during *Shigella* infection in HeLa cells. *Shigella* infection for 4 hours at moi 1000 induces high levels of LDH release. Inhibition of Drp1 with Mdivi-1 as well as Drp1 depletion with siRNA significantly reduced HeLa cell cytotoxicity.

Drp1 is recruited to the mitochondria during apoptosis and programmed necrosis. During apoptosis, pro-apoptotic Bax localises to the outer membrane (OM) of the mitochondria and colocalises with Mfn2 and activates Drp1 at fission sites (Wasiak et al., 2007). Following mitochondrial fragmentation, mitochondrial OM permeabilisation (MOMP) and cristae reorganisation, cytochrome *c* is released and caspases are subsequently activated (Frank et al., 2001). Upon programmed necrosis induction by tumour necrosis factor-α (TNF-α), RIP1 and RIP3 interacts with MLKL (Wang et al., 2012). The RIP1/RIP3/MLKL complex is translocated to the mitochondria to engage mitochondrial protein phosphatase long variant (PGAM5L) initially and subsequently PGAM5S (PGAM short variant) on the mitochondrial membrane. Drp1 GTPase activity is activated via dephosphorylation at Ser637, likely by both PGAM5L and PGAM5S in situ on the mitochondrial OM (Wang et al., 2012). It is speculated Drp1 activation may cause mitochondrial fragmentation resulting in reduced ATP production, ROS generation or other downstream events (Wang et al., 2012).

We next investigated if components of apoptosis or programmed necrosis are activated during *Shigella* infection. HeLa cells treated with STS to induce apoptosis resulted in caspase-3 activation as expected (Nicolier et al., 2009), but no significant LDH release was detected in the culture supernatant. Unsurprisingly pan-caspase inhibition with Z-VAD-fmk or its inactive analogue, Z-FA-fmk did not affect LDH release in *Shigella*-infected HeLa cells. Inhibition of programmed necrosis components such RIP1 and MLKL did not reduce LDH release during *Shigella* infection. ROS and NOS inhibitors also had no effect on LDH release. During *Shigella* infection (moi 500, 3.5 h), mitochondrial fragmentation was observed in ~ 30% of HeLa cells. Mitochondrial fragmentation in infected HeLa cells was halved when Drp1 was inhibited with Mdivi-1 or depleted with siRNA. Previously mitochondrial fragmentation was not observed

when HeLa cells were infected with *Shigella* for 1 h at moi 50 (Stavru et al., 2011). In that study t = 1 h refers to the 1 h infection time prior to incubation with 80 μg/mL gentamicin to remove extracellular bacteria. In our study the equivalent time point is t = 0. Collectively data from the previous study and our observations showed during *Shigella* infection, mitochondrial fragmentation occurs at a later time point and/or at a much higher moi. In spite of the high bacterial load, HeLa cells remain intact and alive, similar to observations reported earlier (Mantis et al., 1996).

Overall our results suggest that at high moi, *Shigella* infection induces non-apoptotic HeLa cell death which is mediated by Drp1 and accompanied by mitochondrial fragmentation. Furthermore HeLa cell death induction during *Shigella* infection is also not dependent on the RIP1/MLKL programmed necrosis pathway. Previously hallmarks of necrosis such as loss of mitochondrial inner potential, nuclear and plasma membrane swelling were observed at 8 h post infection in MEFs infected with *Shigella* (strain M90T) at moi 100 (Carneiro et al., 2009). ROS generation was also observed 10 h post infection (Carneiro et al., 2009). Consistent with previous finding, ROS scavengers had no effect on LDH release at 4 h post infection in this study. Mitochondrial swelling was reported in HaCat cells infected with *S. flexneri* strain YSH6000 at moi 25 for 2 h (Kobayashi et al., 2013). Changes to mitochondrial morphology observed previously might now be attributed to Drp1-mediated mitochondrial fragmentation.

Mitochondrial fission during host cell death in other bacterial infections have been reported, although Drp1 involvment is not essential. The pore-forming vacuolating cytotoxin A (VacA) toxin of the gastric pathogen, *Helicobacter pylori,* recruits and activates Drp1 resulting in mitochondrial fission, Bax activation, MOMP and cytochrome *c* release (Jain et al., 2011). Drp1 fission however is not a prerequisite for VacA-mediated MOMP (Jain et al., 2011). Another pore-forming toxin, listeriolysin O (LLO) from *Listeria monocytogenes*, the causative agent of food-borne listeriosis, was reported to fragment mitochondrial networks in HeLa cells, followed by subsequent decrease in the mitochondrial membrane potential and ATP levels (Stavru et al., 2011). Intriguingly the Drp1 receptor, Mff, is degraded resulting in reduced Drp1 at the mitochondria following *Listeria* infection or LLO treatment but mitochondrial fission is not disrupted (Stavru et al., 2013). It appears the endoplasmic reticulum and the actin cytoskeleton

facilitates mitochondrial fission independent of Drp1, although the exact mechanism is not known.

Earlier we reported dynasore treatment and dynamin II knockdown with siRNA reduced *Shigella* cell spreading in HeLa cells (Lum et al., 2013). Dynasore is a non-competitive, reversible inhibitor of dynamin II and Drp1 GTPase activity. We decided to investigate Drp1's role, if any, in *Shigella* infectious focus and plaque formation. Drp1 inhibition with Mdivi-1 reduced *Shigella* cell spreading in a dose dependant manner and Drp1 knockdown with siRNA also reduced *Shigella* plaque size. Previously Drp1 was reported to colocalise with F-actin stress fibers in Cos-1 cells, an immortalized mammalian fibroblastic cell line (DuBoff et al., 2012). We did not observe any interactions between Drp1 and either the F-actin cytoskeleton or the *Shigella* F-actin tail via IF microscopy in this study. High levels of Drp1 were detected by microscopy in Cos-1 cells (DuBoff et al., 2012), however low levels of Drp1 was observed in HeLa cells in our study. Hence it is possible Drp1 recruitment to HeLa cell F-actin cytoskeleton and/or *Shigella* F-actin tail may not be evident due to technical limitations.

A study in *Potoroo tridactylis* kidney epithelial (PtK2) cells showed that *Listeria* cell spreading in areas with high mitochondrial density (perinuclear region) had increased mean speed and greater curvature in trajectories compared to areas with low mitochondrial density (cell periphery) (Lacayo and Theriot, 2004). *Listeria* and *Shigella* both mediate actin based motility for cell spreading (Gouin et al., 2005). Inhibition of Drp1 forms net-like mitochondrial networks, which can collapse into perinuclear structures (Smirnova et al., 2001; Smirnova et al., 1998). Hence Mdivi-1 treatment would alter the intracellular millieu of HeLa cells dramatically, such that *Shigella* intracellular speed and movement would be adversely affected. In Mdivi-1 treated cells, F-actin comet tail formation, intracellular bacterial growth and protrusion formation was not affected. Hence *Shigella* protrusion formation is not likely to be dependent on its intracellular motility. Lacoya and Theriot (2004) also observed that MitoTracker Red-labeled mitochondria had loss of fluorescent label post *Listeria* collision, presumably due to loss of mitochondrial integrity and transmembrane potential. In this study, we also noticed on some occasions that MitoTracker Red labeling was more intense in uninfected HeLa cells compared to infected cells.

Since Mdivi-1 was able to reduce *Shigella* cell spreading and HeLa cell cytotoxicity, the drug's efficacy was tested in vivo in a murine keratoconjunctivitis (Sereny) model we used previously (Lum et al., 2013). However Mdivi-1 treatment did not ameliorate conjunctivitis, at least under the dosing protocol used in these studies. Since an Δ*icsA* mutant is not pathogenic in this model (Lum et al., 2013), this suggest that Mdivi-1 does not significantly impair intercellular spreading in vivo. It is possible that the dosing regime used here was not sufficient to maintain an effective concentration of drug in vivo.

In conclusion, Drp1 and mitochondrial dynamics play important roles in different aspects of *Shigella* pathogenesis. During *Shigella* infection, mitochondrial fission following cell death pathway activation is important to eliminate infected cells. Furthermore loss of mitochondrial networks disrupts *Shigella*'s ability to mediate cell spreading. Loss of mitochondrial structure may have altered the intracellular movement of *Shigella*. Although *Shigella* protrusion formation was not affected, the inefficient intracellular movement over an extended period of time in the duration of both the infectious focus and plaque assay may retard *Shigella*'s movement from one cell to the next, resulting in reduced infectious focus area and plaque size. Since the conditions used to study cell death and cell spreading differ necessarily in HeLa cell confluency, moi and time of infection, it is difficult to speculate if there are any correlations between cell death, cell spreading and mitochondrial structure. Future work should focus on how Drp1 is recruited and activated during *Shigella* infection and if disruption of mitochondrial dynamics would also affect other bacteria which rely on actin based motility for host dissemination.

Acknowledgements

We are grateful to Dr. Stephen R. Attridge for assistance with the mouse studies. This work is supported by a Program Grant (565526) from the National Health and Medical Research Council (NHMRC) of Australia. ML was the recipient of the Australian Postgraduate Award from the NHMRC.

References

Ashida, H., Mimuro, H., Ogawa, M., Kobayashi, T., Sanada, T., Kim, M., Sasakawa, C., 2011. Cell death and infection: a double-edged sword for host and pathogen survival. J. Cell Biol. 195, 931-942.

562 Bardhan, P., Faruque, A., Naheed, A., Sack, D., 2010. Decrease in Shigellosis-related deaths without
563 *Shigella* spp.-specific interventions, Asia. Emerg. Infect. Dis. 16, 1718-1723.
564 Bergounioux, J., Elisee, R., Prunier, A.-L., Donnadieu, F., Sperandio, B., Sansonetti, P., Arbibe, L., 2012.
565 Calpain Activation by the *Shigella flexneri* Effector VirA Regulates Key Steps in the Formation and Life of
566 the Bacterium's Epithelial Niche. Cell Host & Microbe 11, 240-252.
567 Bernardini, M.L., Mounier, J., d'Hauteville, H., Coquis-Rondon, M., Sansonetti, P.J., 1989. Identification of
568 *icsA*, a plasmid locus of *Shigella flexneri* that governs bacterial intra- and intercellular spread through
569 interaction with F-actin. Proc. Natl. Acad. Sci. U. S. A. 86, 3867-3871.
570 Bishai, E.A., Sidhu, G.S., Li, W., Dhillon, J., Bohil, A.B., Cheney, R.E., Hartwig, J.H., Southwick, F.S., 2012.
571 Myosin-X Facilitates *Shigella*-induced Membrane Protrusions and Cell-to-Cell Spread. Cell. Microbiol. 15,
572 353–367.
573 Carneiro, L.A.M., Travassos, L.H., Soares, F., Tattoli, I., Magalhaes, J.G., Bozza, M.T., Plotkowski, M.C.,
574 Sansonetti, P.J., Molkentin, J.D., Philpott, D.J., Girardin, S.E., 2009. *Shigella* Induces Mitochondrial
575 Dysfunction and Cell Death in Nonmyleoid Cells. Cell Host & Microbe 5, 123-136.
576 Cassidy-Stone, A., Chipuk, J.E., Ingerman, E., Song, C., Yoo, C., Kuwana, T., Kurth, M.J., Shaw, J.T.,
577 Hinshaw, J.E., Green, D.R., Nunnari, J., 2008. Chemical inhibition of the mitochondrial division dynamin
578 reveals its role in Bax/Bak-dependent mitochondrial outer membrane permeabilization. Dev. Cell 14,
579 193-204.
580 Cossart, P., Sansonetti, P.J., 2004. Bacterial Invasion: The Paradigms of Enteroinvasive Pathogens.
581 Science 304, 242-248.
582 Degterev, A., Hitomi, J., Germscheid, M., Ch'en, I.L., Korkina, O., Teng, X., Abbott, D., Cuny, G.D., Yuan,
583 C., Wagner, G., Hedrick, S.M., Gerber, S.A., Lugovskoy, A., Yuan, J., 2008. Identification of RIP1 kinase as
584 a specific cellular target of necrostatins. Nat. Chem. Biol. 4, 313-321.
585 Dodo, K., Katoh, M., Shimizu, T., Takahashi, M., Sodeoka, M., 2005. Inhibition of hydrogen peroxide-
586 induced necrotic cell death with 3-amino-2-indolylmaleimide derivatives. Bioorg. Med. Chem. Lett. 15,
587 3114-3118.
588 DuBoff, B., Götz, J., Feany, Mel B., 2012. Tau Promotes Neurodegeneration via DRP1 Mislocalization
589 In Vivo. Neuron 75, 618-632.
590 Faherty, C.S., Maurelli, A.T., 2009. Spa15 of *Shigella flexneri* Is Secreted through the Type III Secretion
591 System and Prevents Staurosporine-Induced Apoptosis. Infect. Immun. 77, 5281-5290.
592 Ferrari, L.F., Chum, A., Bogen, O., Reichling, D.B., Levine, J.D., 2011. Role of Drp1, a key mitochondrial
593 fission protein, in neuropathic pain. J. Neurosci. 31, 11404-11410.
594 Frank, S., Gaume, B., Bergmann-Leitner, E.S., Leitner, W.W., Robert, E.G., Catez, F., Smith, C.L., Youle,
595 R.J., 2001. The role of dynamin-related protein 1, a mediator of mitochondrial fission, in apoptosis. Dev.
596 Cell 1, 515-525.
597 Friedman, J.R., Lackner, L.L., West, M., DiBenedetto, J.R., Nunnari, J., Voeltz, G.K., 2011. ER Tubules Mark
598 Sites of Mitochondrial Division. Science 334, 358-362.
599 Fukumatsu, M., Ogawa, M., Arakawa, S., Suzuki, M., Nakayama, K., Shimizu, S., Kim, M., Mimuro, H.,
600 Sasakawa, C., 2012. *Shigella* Targets Epithelial Tricellular Junctions and Uses a Noncanonical Clathrin-
601 Dependent Endocytic Pathway to Spread Between Cells. Cell Host Microbe 11, 325-336.
602 Golstein, P., Kroemer, G., 2007. Cell death by necrosis: towards a molecular definition. Trends Biochem.
603 Sci. 32, 37-43.
604 Gouin, E., Welch, M.D., Cossart, P., 2005. Actin-based motility of intracellular pathogens. Curr. Opin.
605 Microbiol. 8, 35-45.
606 Heindl, J.E., Saran, I., Yi, C.-r., Lesser, C.F., Goldberg, M.B., 2009. Requirement for formin-induced actin
607 polymerization during spread of *Shigella*. Infect. Immun. 78, 193–203.

Jain, P., Luo, Z.-Q., Blanke, S.R., 2011. *Helicobacter pylori* vacuolating cytotoxin A (VacA) engages the mitochondrial fission machinery to induce host cell death. Proc. Natl. Acad. Sci. U. S. A. 108, 16032-16037.

Kadurugamuwa, J.L., Rohde, M., Wehland, J., Timmis, K.N., 1991. Intercellular spread of *Shigella flexneri* through a monolayer mediated by membranous protrusions and associated with reorganization of the cytoskeletal protein vinculin. Infect. Immun. 59, 3463-3471.

Kim, H.J., Koo, S.Y., Ahn, B.H., Park, O., Park, D.H., Seo, D.O., Won, J.H., Yim, H.J., Kwak, H.S., Park, H.S., Chung, C.W., Oh, Y.L., Kim, S.H., 2010. NecroX as a novel class of mitochondrial reactive oxygen species and ONOO(-) scavenger. Arch. Pharm. Res. 33, 1813-1823.

Kobayashi, T., Ogawa, M., Sanada, T., Mimuro, H., Kim, M., Ashida, H., Akakura, R., Yoshida, M., Kawalec, M., Reichhart, J.-M., Mizushima, T., Sasakawa, C., 2013. The *Shigella* OspC3 Effector Inhibits Caspase-4, Antagonizes Inflammatory Cell Death, and Promotes Epithelial Infection. Cell Host & Microbe 13, 570-583.

Korobova, F., Ramabhadran, V., Higgs, H.N., 2013. An Actin-Dependent Step in Mitochondrial Fission Mediated by the ER-Associated Formin INF2. Science 339, 464-467.

Lacayo, C.I., Theriot, J.A., 2004. *Listeria monocytogenes* actin-based motility varies depending on subcellular location: a kinematic probe for cytoarchitecture. Mol. Biol. Cell 15, 2164-2175.

Lamkanfi, M., Dixit, V.M., 2010. Manipulation of Host Cell Death Pathways during Microbial Infections. Cell Host & Microbe 8, 44-54.

Lembo-Fazio, L., Nigro, G., Noel, G., Rossi, G., Chiara, F., Tsilingiri, K., Rescigno, M., Rasola, A., Bernardini, M.L., 2011. Gadd45[alpha] activity is the principal effector of *Shigella* mitochondria-dependent epithelial cell death *in vitro* and *ex vivo*. Cell Death & Dis. 2, e122.

Lett, M.C., Sasakawa, C., Okada, N., Sakai, T., Makino, S., Yamada, M., Komatsu, K., Yoshikawa, M., 1989. *virG,* a plasmid-coded virulence gene of *Shigella flexneri*: identification of the *virG* protein and determination of the complete coding sequence. J. Bacteriol. 171, 353-359.

Lum, M., Attridge, S.R., Morona, R., 2013. Impact of Dynasore an Inhibitor of Dynamin II on *Shigella flexneri* Infection. PLoS One 8, e84975.

Makino, S., Sasakawa, C., Kamata, K., Kurata, T., Yoshikawa, M., 1986. A genetic determinant required for continuous reinfection of adjacent cells on large plasmid in *S. flexneri 2a*. Cell 46, 551-555.

Mantis, N., Prévost, M.C., Sansonetti, P., 1996. Analysis of epithelial cell stress response during infection by *Shigella flexneri*. Infect. Immun. 64, 2474-2482.

Morona, R., Daniels, C., Van Den Bosch, L., 2003. Genetic modulation of *Shigella flexneri* 2a lipopolysaccharide O antigen modal chain length reveals that it has been optimized for virulence. Microbiol. 149, 925-939.

Morona, R., Van Den Bosch, L., 2003. Lipopolysaccharide O antigen chains mask IcsA (VirG) in *Shigella flexneri*. FEMS Microbiol. Lett. 221, 173-180.

Murayama, S.Y., Sakai, T., Makino, S., Kurata, T., Sasakawa, C., Yoshikawa, M., 1986. The use of mice in the Sereny test as a virulence assay of Shigellae and enteroinvasive *Escherichia coli*. Infect. Immun. 51, 696-698.

Nicolier, M., Decrion-Barthod, A.-Z., Launay, S., Prétet, J.-L., Mougin, C., 2009. Spatiotemporal activation of caspase-dependent and -independent pathways in staurosporine-induced apoptosis of p53wt and p53mt human cervical carcinoma cells. Biol. Cell. 101, 455-467.

Oaks, E.V., Wingfield, M.E., Formal, S.B., 1985. Plaque formation by virulent *Shigella flexneri*. Infect. Immun. 48, 124-129.

Ong, S.B., Subrayan, S., Lim, S.Y., Yellon, D.M., Davidson, S.M., Hausenloy, D.J., 2010. Inhibiting mitochondrial fission protects the heart against ischemia/reperfusion injury. Circulation 121, 2012-2022.

Otera, H., Ishihara, N., Mihara, K., 2013. New insights into the function and regulation of mitochondrial fission. BBA-Mol. Cell. Res. 1833, 1256-1268.

Otera, H., Wang, C., Cleland, M.M., Setoguchi, K., Yokota, S., Youle, R.J., Mihara, K., 2010. Mff is an essential factor for mitochondrial recruitment of Drp1 during mitochondrial fission in mammalian cells. J. Cell Biol. 191, 1141-1158.

Reed, J.C., 2000. Mechanisms of apoptosis. Am. J. Pathol. 157, 1415-1430.

Sansonetti, P.J., Mounier, J., Prévost, M.C., Mege, R.M., 1994. Cadherin expression is required for the spread of *Shigella flexneri* between epithelial cells. Cell 76, 829-839.

Sansonetti, P.J., Phalipon, A., Arondel, J., Thirumalai, K., Banerjee, S., Akira, S., Takeda, K., Zychlinsky, A., 2000. Caspase-1 activation of IL-1beta and IL-18 are essential for *Shigella flexneri*-induced inflammation. Immunity 12, 581-590.

Sansonetti, P.J., Ryter, A., Clerc, P., Maurelli, A.T., Mounier, J., 1986. Multiplication of *Shigella flexneri* within HeLa cells: lysis of the phagocytic vacuole and plasmid-mediated contact hemolysis. Infect. Immun. 51, 461-469.

Schuch, R., Sandlin, R.C., Maurelli, A.T., 1999. A system for identifying post-invasion functions of invasion genes: requirements for the Mxi-Spa type III secretion pathway of *Shigella flexneri* in intercellular dissemination. Mol. Microbiol. 34, 675-689.

Senerovic, L., Tsunoda, S.P., Goosmann, C., Brinkmann, V., Zychlinsky, A., Meissner, F., Kolbe, M., 2012. Spontaneous formation of IpaB ion channels in host cell membranes reveals how *Shigella* induces pyroptosis in macrophages. Cell Death Dis. 3, e384.

Smirnova, E., Griparic, L., Shurland, D.-L., van der Bliek, A.M., 2001. Dynamin-related Protein Drp1 Is Required for Mitochondrial Division in Mammalian Cells. Mol. Biol. Cell 12, 2245-2256.

Smirnova, E., Shurland, D.-L., Ryazantsev, S.N., van der Bliek, A.M., 1998. A Human Dynamin-related Protein Controls the Distribution of Mitochondria. J. Cell Biol. 143, 351-358.

Stavru, F., Bouillaud, F., Sartori, A., Ricquier, D., Cossart, P., 2011. *Listeria monocytogenes* transiently alters mitochondrial dynamics during infection. Proc. Natl. Acad. Sci. U. S. A. 108, 3612-3617.

Stavru, F., Palmer, A.E., Wang, C., Youle, R.J., Cossart, P., 2013. Atypical mitochondrial fission upon bacterial infection. Proc. Natl. Acad. Sci. U. S. A. 110, 16003-16008.

Sun, L., Wang, H., Wang, Z., He, S., Chen, S., Liao, D., Wang, L., Yan, J., Liu, W., Lei, X., Wang, X., 2012. Mixed lineage kinase domain-like protein mediates necrosis signaling downstream of RIP3 kinase. Cell 148, 213-227.

Suzuki, T., Franchi, L., Toma, C., Ashida, H., Ogawa, M., Yoshikawa, Y., Mimuro, H., Inohara, N., Sasakawa, C., Nunez, G., 2007. Differential regulation of caspase-1 activation, pyroptosis, and autophagy via Ipaf and ASC in *Shigella*-infected macrophages. PLoS Pathog. 3, e111.

Tang, W.X., Wu, W.H., Qiu, H.Y., Bo, H., Huang, S.M., 2013. Amelioration of rhabdomyolysis-induced renal mitochondrial injury and apoptosis through suppression of Drp-1 translocation. J. Nephrol. 26, 1073-1082.

Tran Van Nhieu, G., Clair, C., Bruzzone, R., Mesnil, M., Sansonetti, P., Combettes, L., 2003. Connexin-dependent inter-cellular communication increases invasion and dissemination of *Shigella* in epithelial cells. Nat. Cell Biol. 5, 720-726.

Vandenabeele, P., Galluzzi, L., Vanden Berghe, T., Kroemer, G., 2010. Molecular mechanisms of necroptosis: an ordered cellular explosion. Nat. Rev. Mol. Cell Biol. 11, 700-714.

Wang, Z., Jiang, H., Chen, S., Du, F., Wang, X., 2012. The Mitochondrial Phosphatase PGAM5 Functions at the Convergence Point of Multiple Necrotic Death Pathways. Cell 148, 228-243.

Wasiak, S., Zunino, R., McBride, H.M., 2007. Bax/Bak promote sumoylation of DRP1 and its stable association with mitochondria during apoptotic cell death. J. Cell Biol. 177, 439-450.

Willingham, S.B., Bergstralh, D.T., O'Connor, W., Morrison, A.C., Taxman, D.J., Duncan, J.A., Barnoy, S., Venkatesan, M.M., Flavell, R.A., Deshmukh, M., Hoffman, H.M., Ting, J.P., 2007. Microbial pathogen-induced necrotic cell death mediated by the inflammasome components CIAS1/cryopyrin/NLRP3 and ASC. Cell Host Microbe 2, 147-159.

704 Zheng, W., Degterev, A., Hsu, E., Yuan, J., Yuan, C., 2008. Structure-activity relationship study of a novel
705 necroptosis inhibitor, necrostatin-7. Bioorg. Med. Chem. Lett. 18, 4932-4935.
706
707

Figures

Figure 1. Drp1 mediates *S. flexneri* 2457T-induced HeLa cell death. (A) HeLa cells were infected with *S. flexneri* 2457T (moi 1000) in a 96-well tray for 1 h, followed by incubation with MEM containing 40 µg/mL of gentamicin to exclude extracellular bacteria for 4 h as described in the Methods. LDH release was measured in the presence of DMSO or Mdivi-1. Data are represented as mean ± SEM of independent experiments (n = 3), analysed with one-way ANOVA ($p < 0.0001$), followed by Tukey's post hoc test (*$p < 0.05$, ***$p < 0.001$, ****$p < 0.0001$). No differences in LDH release were observed in the presence of Mdivi-1 or DMSO in the absence of bacterial infection (B - C) HeLa cells were either mock transfected or transfected with control or Drp1 siRNA for 24 h, trypsinised and re-transfected for further 24 h. (B) HeLa cell extracts were probed with anti-Drp1. GAPDH was used as a loading control. (C) Post transfection, HeLa cells were infected with *S. flexneri* 2457T in a 96-well tray as described in (A). Data are represented as mean ± SEM of independent experiments (n = 2), analysed with one-way ANOVA ($p = 0.0129$), followed by Tukey's post hoc test (*$p < 0.05$).

Figure 2. *S. flexneri* 2457T induces non-apoptotic cell death in HeLa cells. HeLa cells were infected with *S. flexneri* 2457T (moi 1000) in a 96-well tray for 1 h, followed by incubation with MEM containing 40 µg/mL of gentamicin to exclude extracellular bacteria for 4 h as described in the Methods. LDH release was measured in the presence of DMSO or (A) Staurosporine (STS) or 0.01% Triton X-100, (B) Z-VAD-fmk, (C) Z-FA-fmk, (D) Necrostatin-1, (E) Necrostatin-7, (F) Necrosulfonamide, (G) IM-54, (H) NecroX-2 or NecroX-5. Data are represented as mean ± SEM of independent experiments (n = 3). (B) - (H) were analysed with one-way ANOVA ($p = 0.0495$ for Z-VAD-fmk, $p > 0.05$ for Z-FA-fmk, $p = 0.0073$ for Necrostatin-1, $p = 0.0458$ for Necrostatin-7, $p > 0.05$ for Necrosulfonamide, $p = 0.0193$ for IM-54, and $p > 0.05$ for NecroX-2 and NecroX-5), followed by Tukey's post hoc test. No differences in LDH release were observed in the presence of the specific chemicals or DMSO in the absence of bacterial infection.

Figure 3. Drp1 inhibition with Mdivi-1 reduces mitochondrial fragmentation in HeLa cells during *S. flexneri* 2457T infection. HeLa cells were infected with *S. flexneri* 2457T (moi 500)

for 1 h, followed by incubation with MEM containing 40 µg/mL of gentamicin to exclude extracellular bacteria for 3.5 h as described in the Methods. Bacteria and HeLa nuclei were stained with DAPI and mitochondria was stained with MitoTracker® Red CMXRos. Images were taken at 100× magnification. Scale bar = 10 µm. The last column is 2.5× magnifications of the respective boxed areas in the MitoTracker® Red CMXRos images. (A) - (F) Uninfected or 2457T-infected HeLa cells were treated with DMSO or Mdivi-1; (A) HeLa; (B) HeLa + DMSO; (C) HeLa + 50 µM Mdivi-1; (D) 2457T; (E) 2457T + DMSO ; (F) 2457T + 50 µM Mdivi-1. (G) The percentage of cells with fragmented mitochondria was determined by counting >100 cells in each experiment. Data are represented as mean ± SEM of independent experiments (n = 2), analysed with one-way ANOVA ($p = 0.0289$), followed by Tukey's post hoc test ($*p < 0.05$).

Figure 4. Transfection of HeLa cells with Drp1 siRNA reduces mitochondrial fragmentation in HeLa cells during *S. flexneri* 2457T infection. HeLa cells were either mock transfected or transfected with control or Drp1 siRNA for 24 h, trypsinised and re-transfected for further 24 h. HeLa cells were infected with *S. flexneri* 2457T (moi 500) for 1 h, followed by incubation with MEM containing 40 µg/mL of gentamicin to exclude extracellular bacteria for 3.5 h as described in the Methods. Bacteria and HeLa nuclei were stained with DAPI and mitochondria was stained with MitoTracker® Red CMXRos. Images were taken at 100× magnification. Scale bar = 10 µm. The last column is 2.5× magnifications of the respective boxed areas in the MitoTracker® Red CMXRos images. (A) - (C) Mock, control siRNA and Drp1 siRNA transfected HeLa cells were infected with 2457T; (A) Mock transfected; (B) Control siRNA; (C) Drp1 siRNA. (D) The percentage of cells with fragmented mitochondria was determined by counting >100 cells in each experiment. Data are represented as mean ± SEM of independent experiments (n = 2), analysed with one-way ANOVA ($p < 0.0001$), followed by Tukey's post hoc test ($*p < 0.05$).

Figure 5. Drp1 inhibition with Mdivi-1 reduces *S. flexneri* MLRM107 foci counts and foci area. HeLa cells were infected with *S. flexneri* MLRM107 in an infectious focus assay using a 12-well tray as described in the Methods. Infectious foci were imaged 24 h post gentamicin treatment. (A) Images shown are overlay of an image taken with phase contrast and TxRed filter (10× magnification). The area of the infectious focus i.e. area where mCherry was detected, is

outlined. Scale bar = 0.1 mm. (B) The total foci counts from one well or (C) mean foci area from one well were calculated. Data are represented as mean ± SEM of independent experiments (n = 3), analysed with one-way ANOVA ($p = 0.0013$ for foci counts and $p = 0.0003$ mean foci area), followed by Tukey's post hoc test (*$p < 0.05$, **$p < 0.01$, ***$p < 0.001$).

Figure 6. HeLa cells transfected with Drp1 siRNA reduces *S. flexneri* 2457T plaque size. HeLa cells were either mock transfected or transfected with control or Drp1 siRNA for 24 h, trypsinised and re-transfected for further 24 h. HeLa cells were infected with *S. flexneri* 2457T in a plaque assay using a 6-well tray as described in the Methods. (A) Wells were stained with Neutral Red to makes plaques more visible. Scale bar = 2 mm. (B) The total plaque counts or (C) mean plaque diameters from each well infected with *Shigella* were calculated. Data are represented as mean ± SEM of independent experiments (n = 2), analysed with one-way ANOVA ($p > 0.05$ for plaque counts and $p = 0.0239$ mean plaque diameters), followed by Tukey's post hoc test (*$p < 0.05$).

Figure 7. *S. flexneri* 2457T protrusion is not affected in the presence of Mdivi-1. HeLa cells were infected with *S. flexneri* 2457T for 1 h in a 24-well tray. HeLa cells were washed thrice with D-PBS and incubated with MEM containing 40 μg/mL of gentamicin (t=0) to exclude extracellular bacteria. Concurrently HeLa cells were treated with 50 μM Mdivi-1 or DMSO for 1.5 h. At t = 1.5, HeLa cells were fixed to observe bacteria protrusions. (A) Infected HeLa cells were imaged at 40× magnification. Scale bar = 10 μm. The arrows indicate protrusion formation. Insert shows 2× enlargement of the indicated region. (B) The percentage of infected cells with bacteria protrusion(s) were enumerated by counting >100 cells in each independent experiment. Data are represented as mean ± SEM of independent experiments (n = 2), analysed with one-way ANOVA ($p > 0.05$).

Figure 8. Drp1 is not localised to the *S. flexneri* 2457T F-actin tails. HeLa cells were infected with *S. flexneri* 2457T in an invasion assay as described in the Methods. Bacteria and HeLa nuclei were stained with DAPI (blue), F-actin was stained with FITC-phalloidin (green) and Drp1 was stained with anti-Drp1 and Alexa Fluor 594-conjugated secondary antibody (red). Images were taken at 100× magnification. Scale bar = 10 μm. (A) - (D) HeLa cells were treated

800 with DMSO, Mdivi-1 or were transfected with Drp1 siRNA and were infected with *S. flexneri*
801 2457T; (A) Untreated; (B) 1% DMSO; (C) 50 μM Mdivi-1; (D) Drp1 siRNA transfected HeLa
802 cells. Arrows indicate F-actin comet tails. The experiment was repeated twice and representative
803 images are shown.
804

828

829

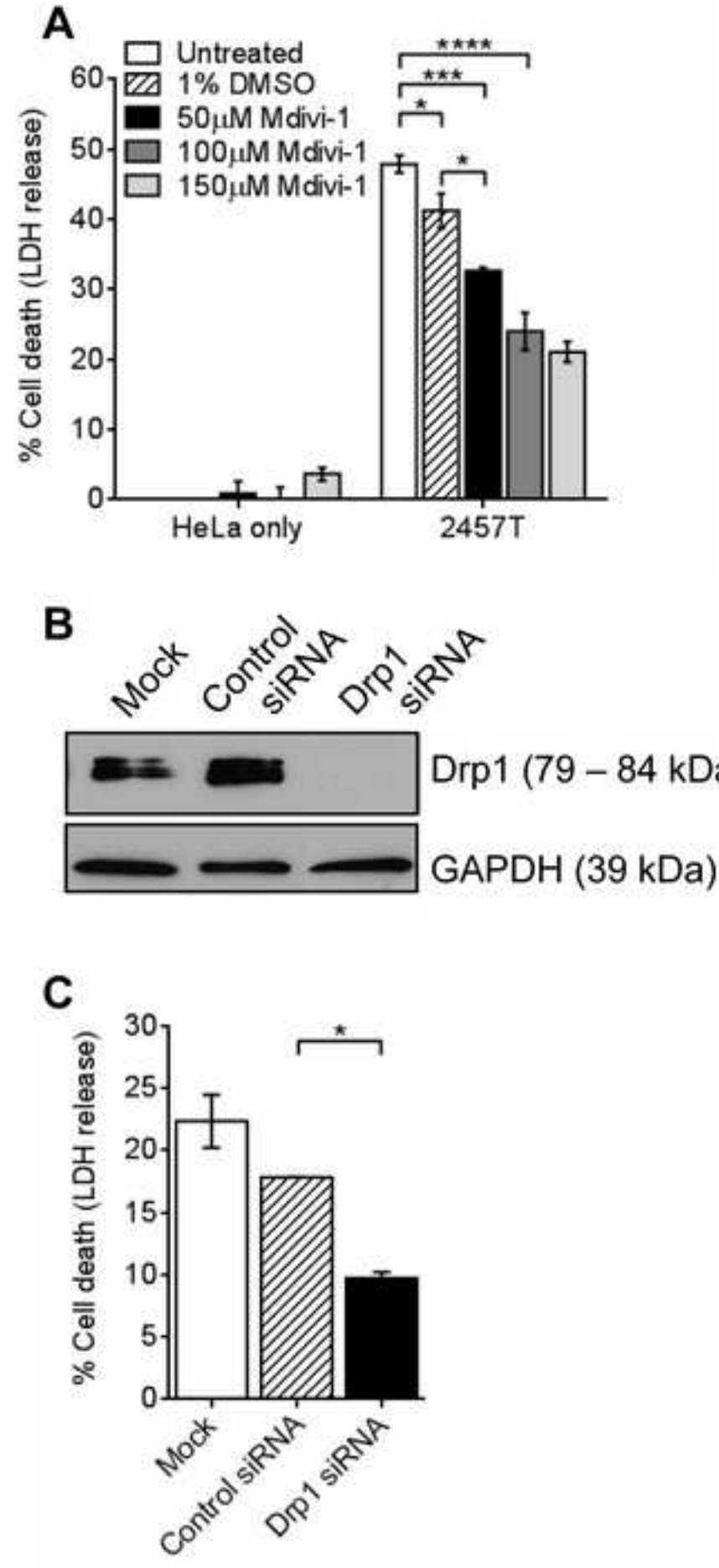

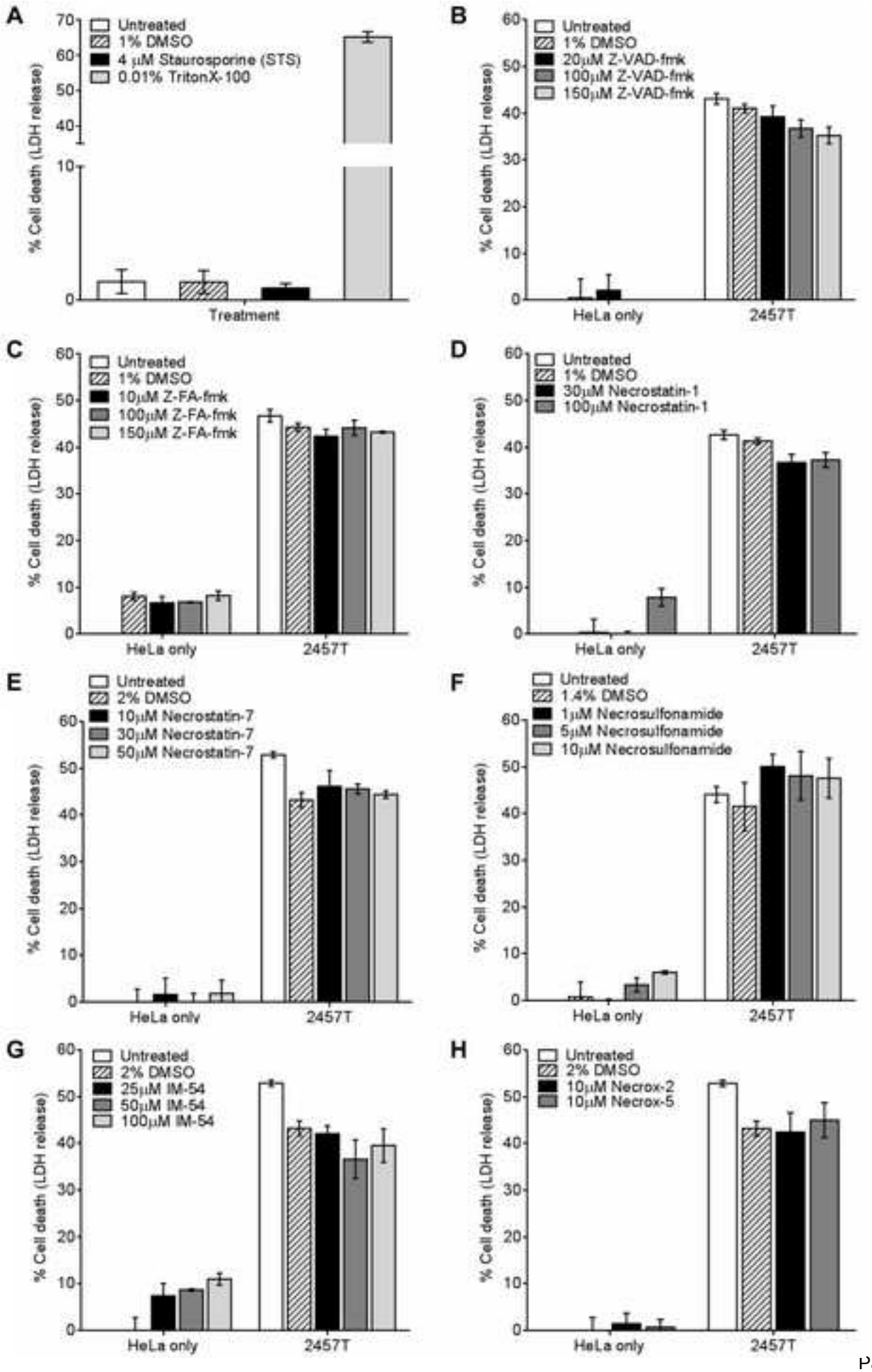

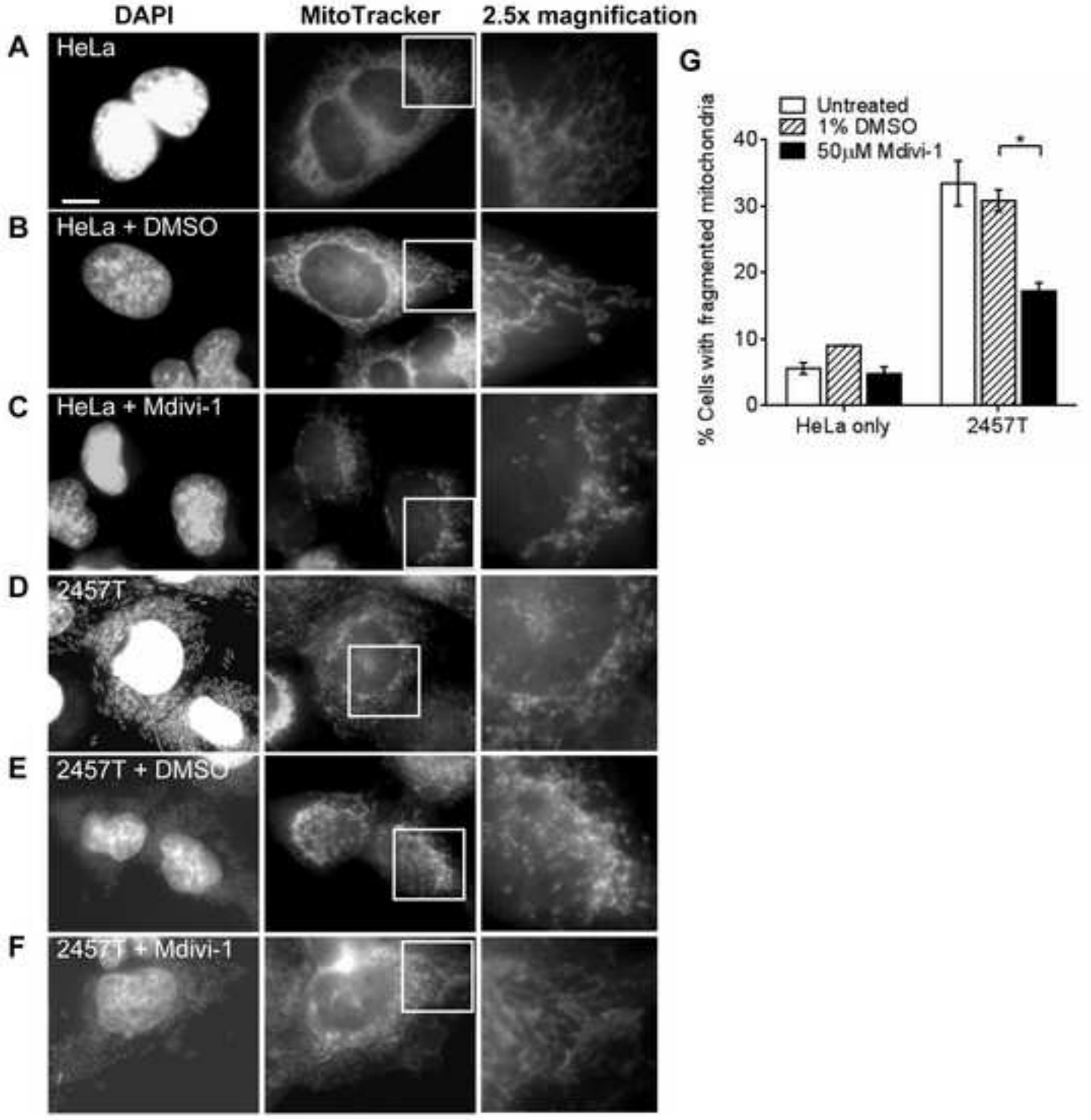

Figure 4

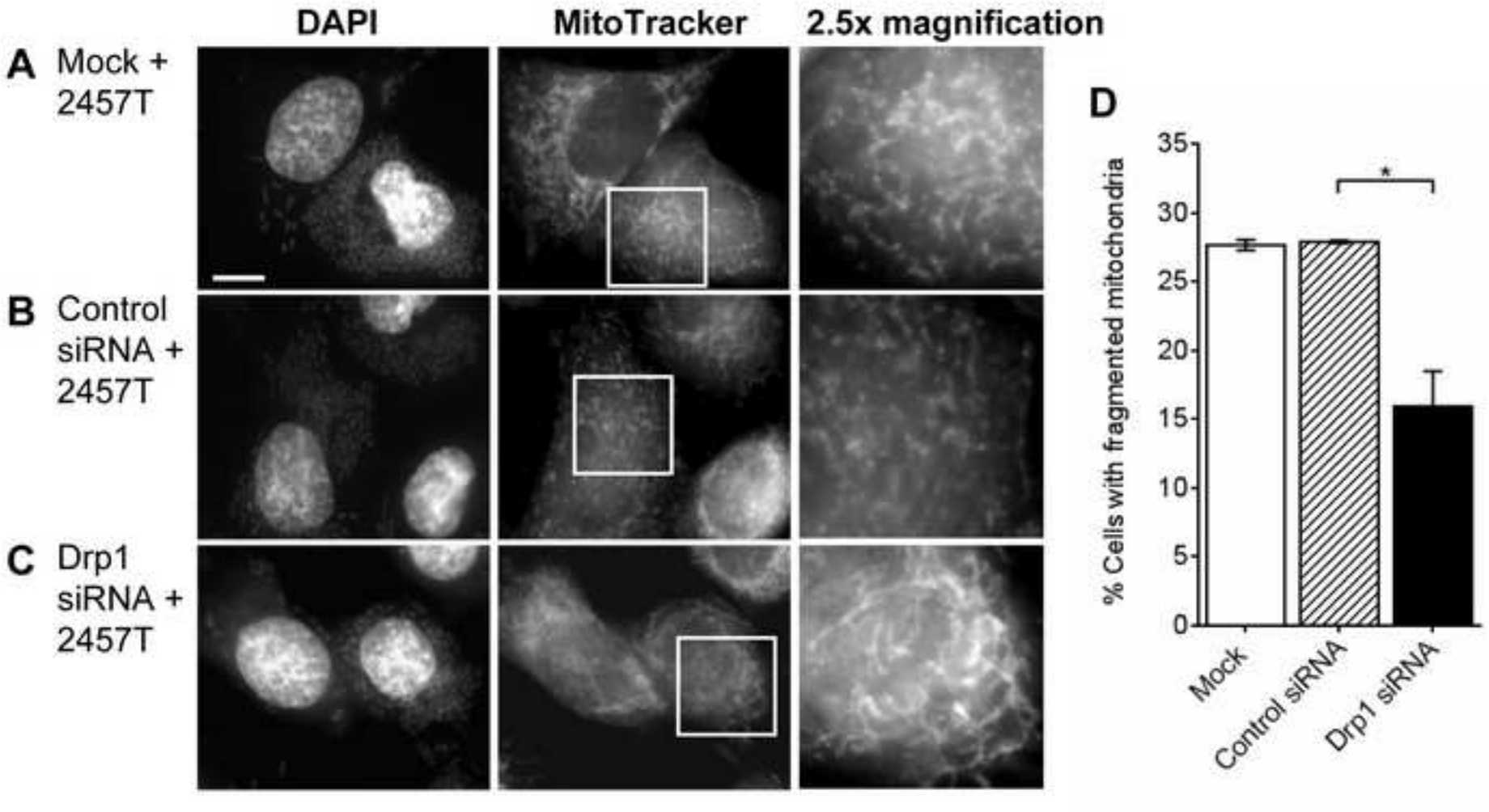
DAPI
MitoTracker
2.5x magnification
A Mock + 2457T
B Control siRNA + 2457T
C Drp1 siRNA + 2457T
D
% Cells with fragmented mitochondria
35
30
25
20
15
10
5
0
*
Mock
Control siRNA
Drp1 siRNA

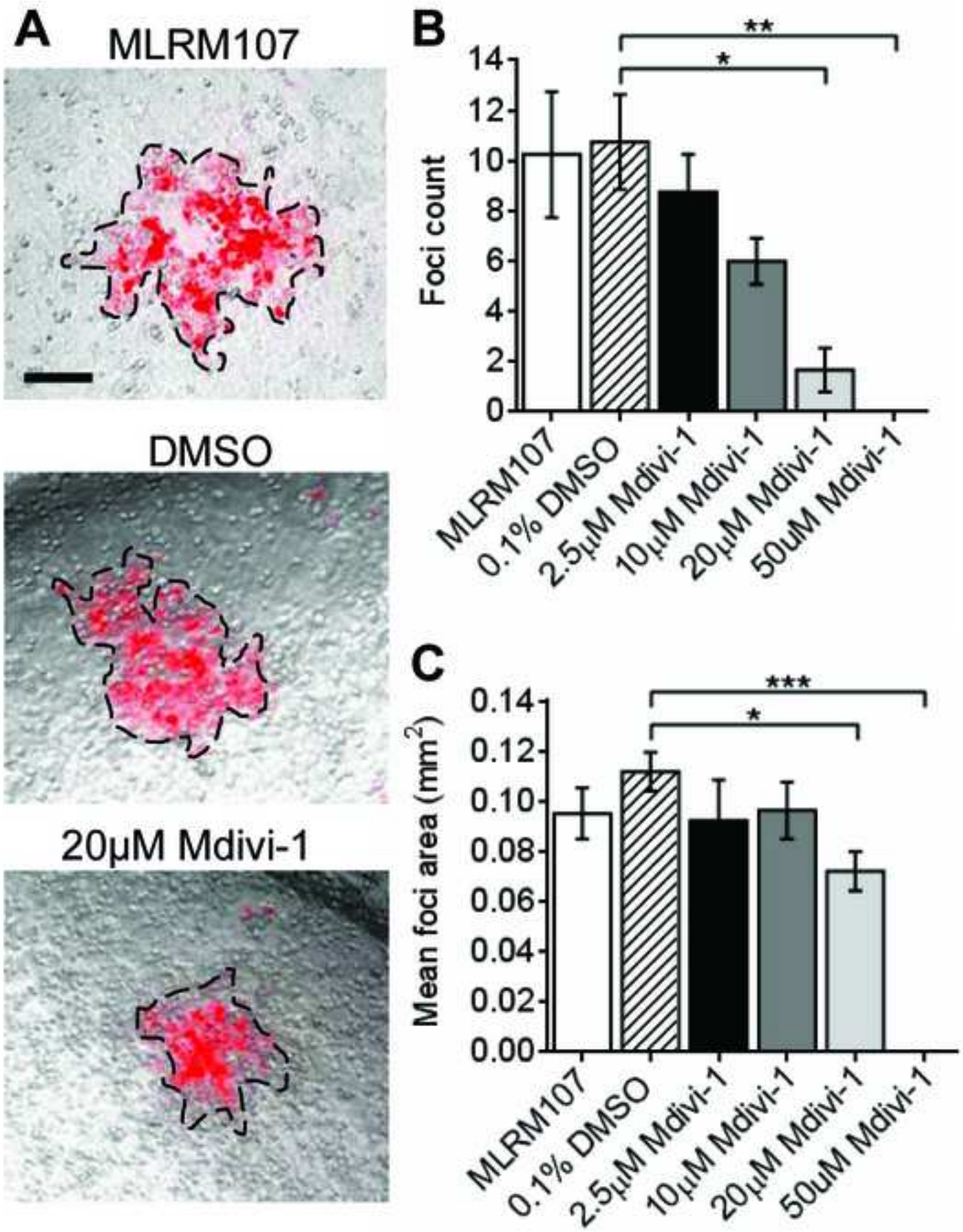

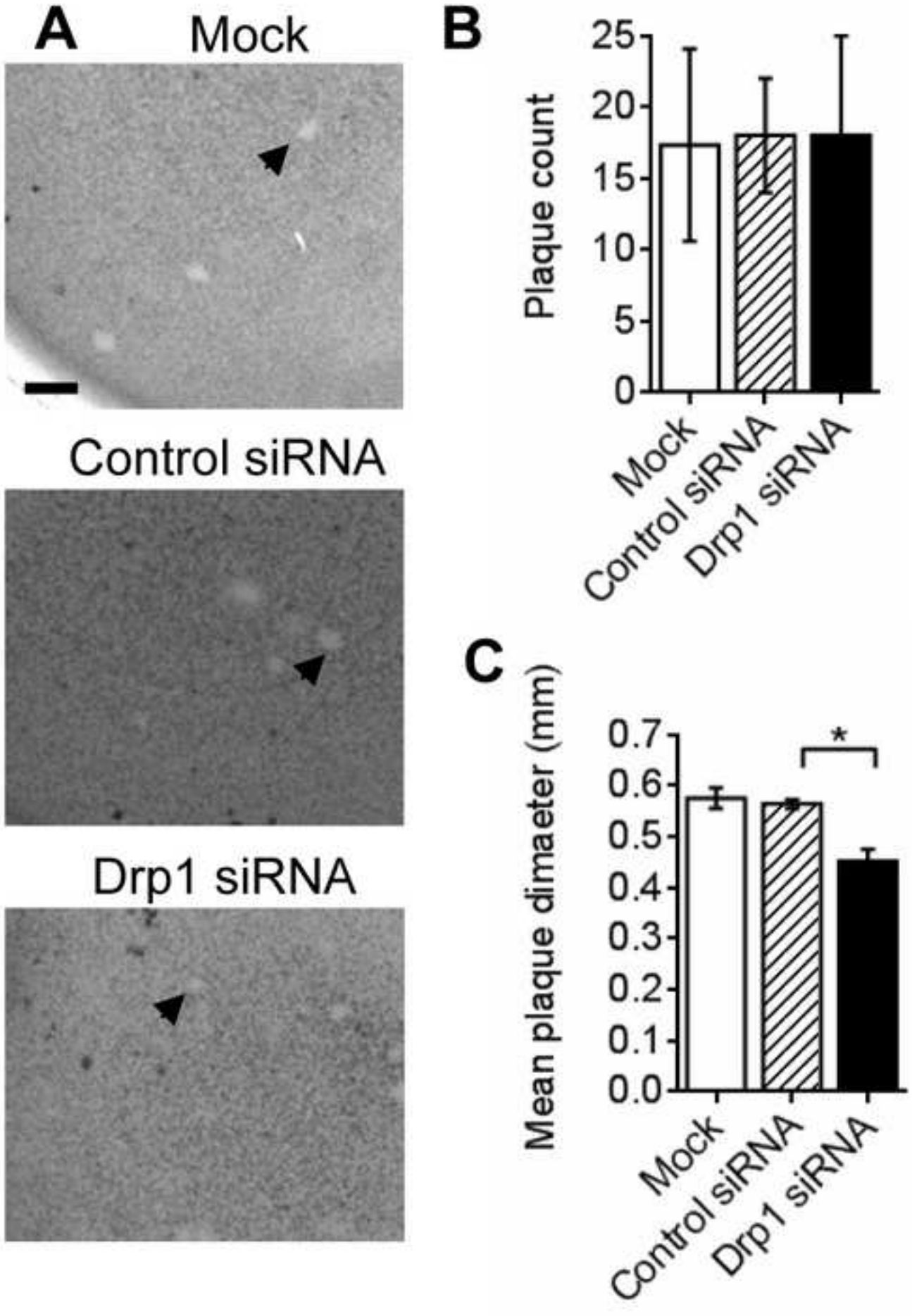

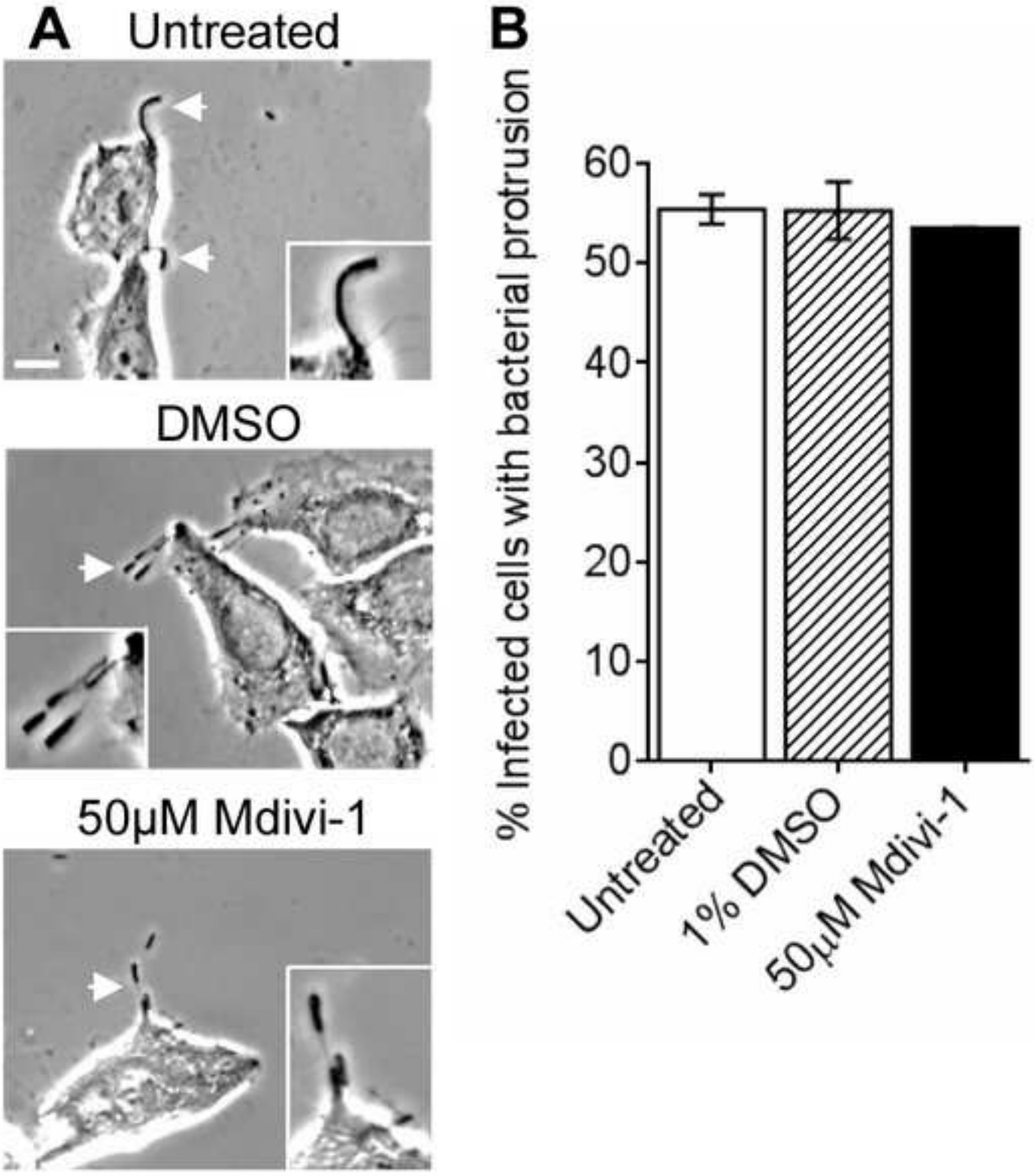

Figure 8

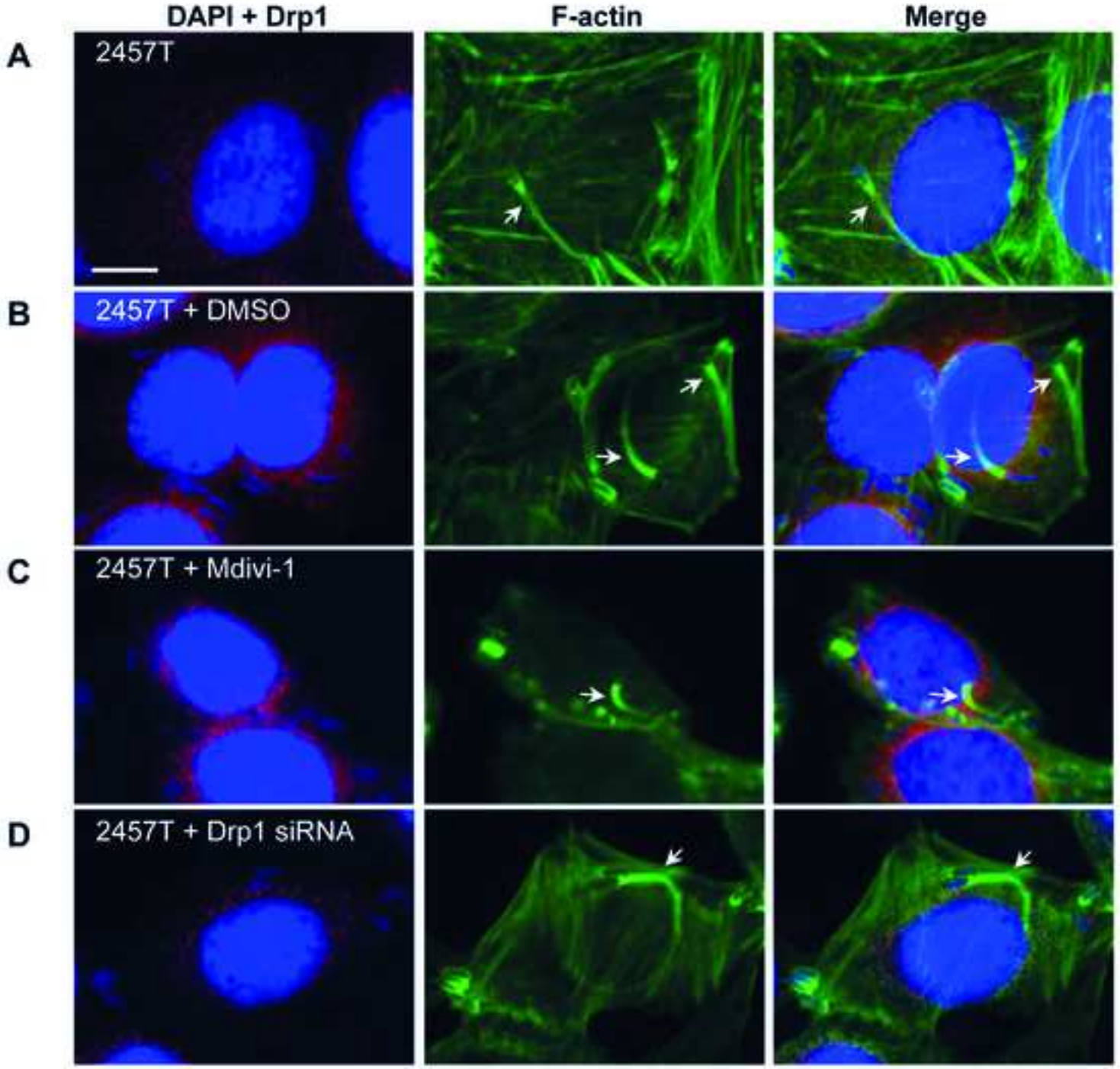
DAPI + Drp1
F-actin
Merge
A
2457T
B
2457T + DMSO
C
2457T + Mdivi-1
D
2457T + Drp1 siRNA

Table 1. Bacterial strains

Strain	Relevant characteristics[#]	Reference or source
S. flexneri		
2457T	*S. flexneri* 2a wild type	Laboratory collection
MLRM107	2457T [pMP7604; Tc^R]	(Lum et al., 2013)
RMA2159	Virulence plasmid-cured 2457T	Laboratory collection

Tet^R, Tetracycline resistant

Lum, M., Attridge, S.R., Morona, R., 2013. Impact of Dynasore an Inhibitor of Dynamin II on *Shigella flexneri* Infection. PLoS One 8, e84975.